Lab on a Chip

Cite this: *Lab Chip*, 2011, **11**, 4207

www.rsc.org/loc

PAPER

Microchip integrating magnetic nanoparticles for allergy diagnosis†

Bruno Teste,[a] Florent Malloggi,[b] Jean-Michel Siaugue,[a] Anne Varenne,[a] Frederic Kanoufi[a] and Stéphanie Descroix*[a]

Received 26th August 2011, Accepted 4th October 2011
DOI: 10.1039/c1lc20809h

We report on the development of a simple and easy to use microchip dedicated to allergy diagnosis. This microchip combines both the advantages of homogeneous immunoassays *i.e.* species diffusion and heterogeneous immunoassays *i.e.* easy separation and preconcentration steps. *In vitro* allergy diagnosis is based on specific Immunoglobulin E (IgE) quantitation, in that way we have developed and integrated magnetic core–shell nanoparticles (MCSNPs) as an IgE capture nanoplatform in a microdevice taking benefit from both their magnetic and colloidal properties. Integrating such immunosupport allows to perform the target analyte (IgE) capture in the colloidal phase thus increasing the analyte capture kinetics since both immunological partners are diffusing during the immune reaction. This colloidal approach improves 1000 times the analyte capture kinetics compared to conventional methods. Moreover, based on the MCSNPs' magnetic properties and on the magnetic chamber we have previously developed the MCSNPs and therefore the target can be confined and preconcentrated within the microdevice prior to the detection step. The MCSNPs preconcentration factor achieved was about 35 000 and allows to reach high sensitivity thus avoiding catalytic amplification during the detection step. The developed microchip offers many advantages: the analytical procedure was fully integrated on-chip, analyses were performed in short assay time (20 min), the sample and reagents consumption was reduced to few microlitres (5 μL) while a low limit of detection can be achieved (about 1 ng mL^{-1}).

Introduction

Allergy has become a major public health issue as it concerns 30% of the population in western countries.[1] Since the discovery of immunoglobulin E (IgE) and its key role in allergic reactions, a growing interest has been observed in developing analytical methods dedicated to IgE quantitation.[2] In clinical research, *in vitro* allergy diagnosis is based on IgE quantitation from patient sera using enzyme-linked immunosorbent assay (ELISA) with a microtiter plate. However ELISA is labor-intensive, time consuming due to mass transfer limitation and requires large volumes of samples and reagents. To tackle these problems, different commercial systems have been developed like immunocap (Phadia), Immulite (Siemens) or Lab on CD (HSG-IMIT), these systems are fully automated, allow high throughput analysis but require specific, large and expensive apparatus as well as high volume of sample and long analysis time. In parallel, some groups have evidenced the interest of microfluidics scale for allergy diagnosis using the microarray format[3] or the Western Blot approach.[4]

The combination of immunoassays and microfluidics led to (i) the integration of the whole lab process, (ii) the handling of low volumes and (iii) the increase of the surface to volume ratio (S/V) while decreasing diffusion distances. The simplest approach consists in performing the immunoassay on the microchannel surface.[5–7] Despite the size reduction to the micrometre scale, the reaction kinetics was still limited by diffusion, in that way different strategies were developed to increase target capture efficiency like flow confinement,[8] chaotic mixer,[9] or electrophoretic preconcentration.[10] In parallel, the integration of microbeads in a microchip allows to improve the S/V and to reduce the diffusion distances.[11–14] Sato *et al.*[15] developed an ELISA on the surface of polystyrene beads packed against a physical restriction thus shortening the total assay time to 40 min while keeping great sensitivity using thermal lens microscopy. Magnetic beads were also used as immunosupport,[16,17] the application of external magnetic field gives access to beads migration[18] and orientation in the microchannel. Gijs *et al.*[19] developed an immunoassay using column configuration thus reducing the quantity of beads and improving sample perfusion. Nevertheless, despite these advantages, the immune reactions were still performed in a heterogeneous format because in many cases the micrometric beads are physically packed or magnetically trapped; their

[a]*Physicochimie des Electrolytes, Colloïdes et Sciences Analytiques (PECSA), UMR 7195 CNRS-ESPCI-ENSCP, France. E-mail: stephanie.descroix@espci.fr*
[b]*MMN, UMR 7083, Gulliver CNRS-ESPCI, Paris, France*
† Electronic supplementary information (ESI) available. See DOI: 10.1039/c1lc20809h

surfaces are thus not totally exploited. Some groups have overcome the problems related to the sedimentation of micrometric beads by performing the analysis with a continuous flow protocol[20] or using a sophisticated fluidic handling and mixing step.[21,22]

Lately, nanoparticles (NPs) and nanowires were largely used for bioanalysis since they provide optical, electrical and magnetic properties. In that way they were mostly used in labeled technologies for rapid and ultra-sensitive detection[23–27] but also as immune capture support.[28–34] Colloidal gold or magnetic NPs appeared as a great candidate for immune support since they offer diffusing properties and a much higher surface to volume ratio. Mayilo *et al.*[35] used the optical properties of gold NPs to develop an immunoassay based on Fluorescence Resonance Energy Transfer (FRET), the LOD was in the range of ng mL^{-1} but this technique suffers from high background signal. Gold NPs were also used in passive agglutination in which the presence of analyte creates clusters determined by dynamic light scattering (DLS) but the assay time was quite long (1 h).[36] In order to improve agglutination kinetics, magnetic NPs were used as immune support by Baudry *et al.* In this case magnetic NPs were forced to collide and the contact time was improved thus shortening the assay time to 5 min. Some commercial devices were also based on magnetic NPs, Philips developed a system (Magnotech) where the target is captured on magnetic NPs and magnetically concentrate on a surface before the detection step. In these cases the detection, based on scattering measurements or total internal reflection, was performed off chip as the integration of such measurement devices is complicated and requires specific materials.[37]

Thus the colloidal NPs based immunoassays were widely developed off chip but the combination of sub 100 nm immunosupport and microfluidic was less exploited. Most of the time, gold NPs[38,39] or quantum dots[40,41] are used as on-chip sensors. Herein, we report on the development of a microchip dedicated to allergy diagnosis that combines the advantages of both homogeneous and heterogeneous immunoassays; in particular, the diffusion of immunological partners and an increase in S/V that should improve analyte mass transfer as well as the integration of a preconcentration step. To do so magnetic core–shell nanoparticles (MCSNPs) have been synthesized and grafted by an antigen to be used as the colloidal immunosupport. Thereafter the whole immunoassay was performed on chip; the target is first captured at the surface of MCSNPs in the colloidal phase. Then the MCSNPs and consequently the target are confined and preconcentrated in a previously developed magnetic chamber prior to the detection step. The influence of MCSNPs concentration and colloidal stability has been evaluated on assay sensitivity using a model target analyte. Then, the kinetics rate of each incubation step was determined. Finally the clinical applicability of the developed microdevice has been evidenced using real sera sample from allergic patient.

Materials and methods

Microsystem fabrication and set up

The microdevice was fabricated in two main steps: master fabrication and replica molding. Master fabrication was performed using the standard multilayer soft lithography method.[42,43] The microstructures (channel and restriction) were designed in a computer aided design (CAD) program. Transparencies of the CAD-generated patterns were then created using commercial services. The first layer was obtained by spin coating the negative SU-8 2002 photoresist (Microchem, viscosity 7.5cSt) at 2000 rpm. The manufacturer predicts a layer height of 2.4 μm. The restriction design was insulated (435 nm, 7 s) onto the wafer and then developed. We measured the height of the restriction with a stylus profiler Dektak4M (Veeco). The measured restriction height (3 μm) was in good agreement with the photoresist manufacturer prediction. On the same wafer we spin coated the second layer. We used the negative SU-8 2015 photoresist (Microchem, viscosity 1250cSt) at 1500 rpm. The channel design was then aligned, with a mask aligner MJB4 (SUSS MicroTec), onto the restrictions and then insulated (435 nm, 10 s). The wafer was developed and the height was measured. The second layer height is approximately 30 μm. The polydimethylsiloxane Sylgard 184 elastomer (PDMS, Dow Corning) was poured and further cured on a SU-8 mold (Microchem). Holes were punched for the inlets and the PDMS replicates were sealed to glass slides following oxygen plasma treatment at 200 mTorr for 30 s using a plasma cleaner (Harrick scientific).

Spherical iron beads (7 ± 0.6 μm, Good Fellow) offering a saturation magnetization of about 1.1×10^6 A m^{-1} were used for the magnetic chamber development (Fig. 1a and b). The iron beads were magnetized with a permanent magnet (Chen Yang, 2 cm diameter and 1 cm high) presenting a magnetic remanence of 1.3 T. The formation of the magnetic beads plug was performed under a sufficient flow rate in order to avoid the iron beads sedimentation. The samples were injected using syringes of different volumes. The latter were connected to the microsystem inlet by a capillary tube. The flow rate was controlled by a syringe pump (Kd scientific).

Microchip analyses were monitored by an IX-71 inverted fluorescence microscopic system (Olympus) equipped with spectral filters, 460–490 nm and a 100 W mercury lamp (Olympus). A CCD camera 1388 × 1038 pixels Pike (RD Vision) was mounted on the microscope and Hiris software (RD Vision) was used for camera control and image processing.

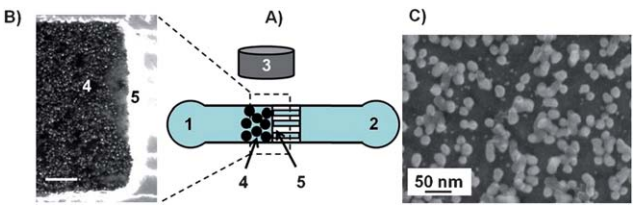

Fig. 1 (A) Chip made of a single channel 1.5 cm long, 200 μm width and 30 μm height with a permanent magnet on the top of the channel. 1: inlet, 2: outlet, 3: external permanent magnet. (B) Top picture of the magnetic chamber observed with photonic microscopy, scale bar: 100 μm (magnitude 100×). 4: ferromagnetic iron beads, 5: physical restriction made of tunnels of 25 μm width and 3 μm height. (C) Scanning electron microscopy of MCSNPs (magnitude 250 000×). Nonencapsulated silica nuclei were observed.

Magnetic core–shell nanoparticles synthesis

Magnetic core–shell nanoparticles are shown in Fig. 1c and their synthesis has been previously reported.[44] Briefly, maghemite nanoparticles (mean physical diameter of 7 nm) were prepared by co-precipitation of Fe^{2+} and Fe^{3+} ions under alkaline conditions. Nanoparticles were coated by citrate anions and dispersed in water. These maghemite nanoparticles were encapsulated in silica shells prepared by condensation of tetraethoxyorthosilicate (TEOS, Sigma), in ethanolic medium in the presence of ammonia as catalyst. The silica shell functionalization was carried out by simultaneous condensation of a silica amine-derived compound (APTS, Sigma) and a silica polyethyleneglycol (PEG)-derived compound (PEOS, Gelest). The concurrent addition of a small amount of TEOS resulted in the formation of a cross-linked silica shell. The particle surface chemistry can be tuned by varying the PEOS to APTS molar ratio, the amount of PEOS remains constant while the quantity of APTS increases. The ratio used here was a 3 : 1 PEOS/APTS ratio. The reaction of silica condensation was carried out overnight and the particle suspension was destabilized with diethyl ether. A red pellet was formed and separated by magnetic settling. The pellet was washed twice with a mixture of diethyl ether and ethanol (15 : 1) and redispersed in 10 mM 3-morpholinopropane-1-sulfonic acid (MOPS, Sigma) buffer (pH 7.5). This colloidal solution of amino-PEG functionalized MCSNPs (approximately 3.3×10^{14} MCSNPs mL^{-1}) was stable for months.

Grafting of α-lactalbumin antigen on magnetic core–shell nanoparticles

The optimization of α-lactalbumin (α-lac, Sigma) antigen grafting *via* a chemometric approach was previously reported.[45] Briefly 350 μL of MCSNPs solution (3.3×10^{14} MCSNP mL^{-1}) were mixed with 200 μL of *N*-(3-dimethylaminopropyl)-*N*-ethylcarbodiimide hydrochloride (EDC, Sigma) at 0.42 mg mL^{-1}, 200 μL of *N*-hydroxysulfosuccinimide sodium salt (NHS, Sigma) at 0.80 mg mL^{-1} and 400 μL of α-lac solution (1 mg mL^{-1},Sigma) in a 2 mL Eppendorf tube. Each reagent solution was freshly prepared in 10 mM MOPS buffer at pH 7.5. All tubes were gently shaken at 20 °C for 15 h. The MCSNPs grafted with α-lac (MCSNPs-Ag) were rinsed 3 times with 400 μL of 10 mM MOPS buffer using centrifugation (15 000*g* per 5 min) or a MACS separator column (Miltenyi). Finally, MCSNPs-Ag were solubilized in 400 μL of 150 mM phosphate buffer salt (PBS)-Tween 0.1% (v/v) using ultrasonic wave for 30 s to facilitate MCSNPs solubilization and prevent any cluster formation.

Immunoassay procedure using the microtiter plate

A microplate with 96 wells (Nunc) was coated with 100 μL of a 5 μg mL^{-1} α-lac solution prepared in 10 mM MOPS buffer for 15 h at 4 °C. Each well was emptied and 200 μL of 150 mM PBS-Tween (0.1% v/v, Sigma) containing polyvinylpyrrolidone (1% w/v, Sigma) were used as the blocking agent (2 h incubation). Then, 100 μL of Goat anti-α-lac IgG (AbI, GeneTex) solution prepared in 150 mM PBS-Tween (0.1% w/v) at various concentrations (0.1 to 10 000 ng mL^{-1}) were added to each well (2 h incubation). 200 μL of 150 mM PBS-Tween (0.1% w/v) were used 3 times for the washing step. Then, 100 μL of 100 μg mL^{-1} AlexaFluor488 labeled anti-AbI (AbII*, GeneTex) prepared in 150 mM PBS-Tween (0.1% w/v) were added. After 1 h incubation, the plate was washed 3 times to remove unbound antibodies and detection was performed exciting AbII* at 488 nm and fluorescent emission was read at 520 nm.

IgE determination in serum was carried out by adding 100 μL of 5 times diluted serum from cow's milk allergic patient (3 h incubation) in a microplate well previously coated with α-lac. After the washing step, 100 μL of alkaline phosphatase labeled anti-human IgE (anti-IgE-AP, Sigma) at 1 μg mL^{-1} was then added for 2 h incubation. Finally 100 μL of *p*-nitrophenyl phosphate (pNPP, Sigma) substrate at 1 mg mL^{-1} were added for 30 min after the rinsing step. The colored product was measured at 405 nm.

Immunoassay using the microchip

The immunoassay in the microchip was performed through two different approaches. In the first one the target AbI capture occurred in the colloidal phase and AbII* interaction occurred in the heterogeneous phase within the magnetic chamber (1st approach) as shown in Fig. 2. In the second approach both the target AbI and AbII* interact successively in the heterogeneous phase with confined MCSNPs within the magnetic chamber (2nd approach).

In the 1st approach, 100 μL of MCSNPs-Ag (1.6×10^{11} MCSNP mL^{-1} final concentration) were mixed with 50 μL of target AbI (various concentrations) then injected into the microchannel where immune reaction was performed in stop flow. After 5 min incubation, permanent magnet (200 mT on its surface) was put at 0.5 cm from the top of the channel and a flow rate of 30 μL h^{-1} was applied for 10 min (for a magnetic plug of 300 μm long, 200 μm width and 30 μm high) to magnetically trap and concentrate MCSNPs in the magnetic chamber. The microchannel was washed for 2 min with 150 mM PBS-Tween (0.1% w/v) at a flow rate of 30 μL h^{-1} and 100 μg mL^{-1} of AbII* were injected at 30 μL h^{-1} for 5 min. After 2 min washing, detection was performed by exciting AbII* and measuring fluorescent emission on a magnetic chamber surface of 20×20 μm^2.

In the 2nd approach, the magnetic chamber was saturated with MCSNPs in the presence of the external magnet and the target AbI was injected at various concentrations for 5 min at 30 μL h^{-1}. The microchannel was washed for 2 min with 150 mM PBS-Tween (0.1% w/v) at a flow rate of 30 μL h^{-1} and 100 μg mL^{-1} of AbII* were injected at 30 μL h^{-1} for 5 min. The detection was performed as previously mentioned.

IgE determination was performed using the 1st approach: 20 μL of serum were mixed with 80 μL of MCSNPs-Ag (6.7×10^{11} MCSNPs mL^{-1} final concentration) and injected into the microchannel. After 5 min incubation in stop flow, the permanent magnet was put on the top of the microdevice and a flow rate of 30 μL h^{-1} was applied for 10 min. After 2 min washing with 150 mM PBS-Tween (0.1% w/v) 100 μg mL^{-1} of FITC labeled anti-human IgE (anti-IgE-FITC, GeneTex) were injected for 5 min at 30 μL h^{-1}. After rinsing, anti-IgE-FITC was detected as described above.

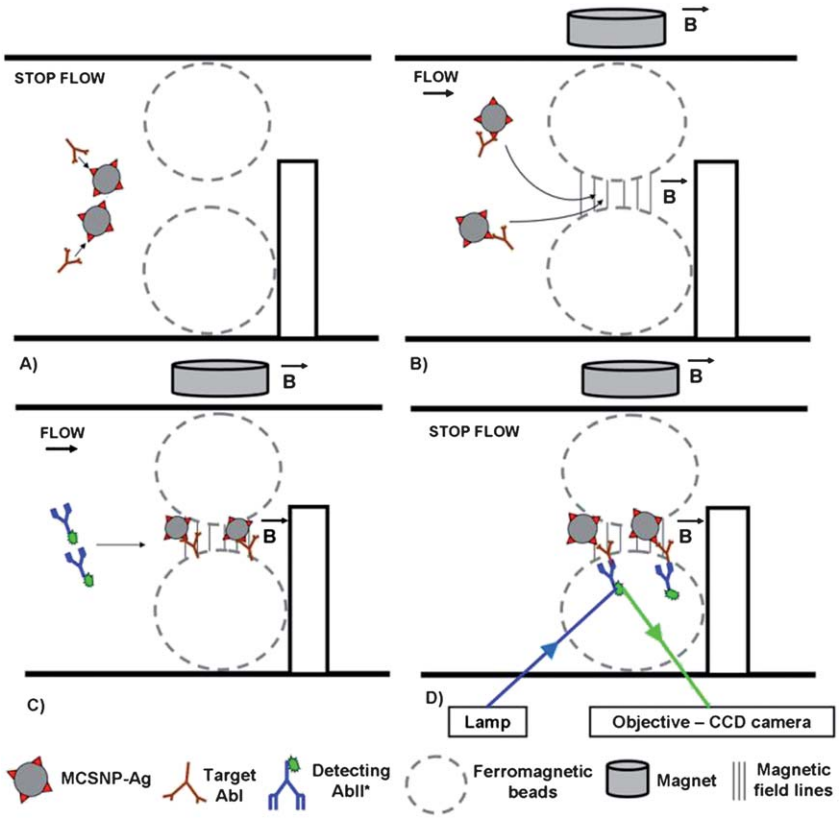

Fig. 2 Principle of the MCSNPs-based immunoassay in the chip. (A) Capture of the target AbI in the colloidal phase and stop flow using MCSNPs-Ag as immunosupport. (B) Application of an external permanent magnet (200 mT on its surface) on the top of the chip with a flow rate of 30 μL h^{-1}. MCSNPs are magnetically trapped and concentrated in the magnetic chamber. (C) AbII* was injected at a flow rate of 30 μL h^{-1} and interacted with the preconcentrated target AbI in the heterogeneous phase within the magnetic chamber. (D) AbII* was excited with a mercury lamp and the fluorescence signal was collected by a charge-coupled device (CCD) camera mounted on an inverted microscope and treated with Hiris software. The fluorescence was measured in the central area (20 × 20 μm^2) of the magnetic chamber.

Results and discussion

The developed system was based on the combination of microfluidic and NPs dedicated to allergy diagnosis. In this respect, magnetic core–shell nanoparticles (MCSNPs) have been designed[44] and characterized[46,47] to be used as immunosupport in a microchip that integrates the whole immunoassay procedure: incubation, preconcentration and detection steps. The choice of MCSNPs as the immunosupport was mainly motivated by their colloidal behavior and Brownian motion, which enhance liquid stirring and favor molecular diffusivity.[48] The MCSNPs (physical diameter of 35 nm) used in this work were made of a magnetic core encapsulated in a silica shell. Recently, their potential for drug delivery has been demonstrated.[49] The surface chemistry of the MCSNPs can be easily tuned as a function of the analytical requirements. In this case, their surface was functionalized with amino moieties to immobilize biomolecules and with polyethylene glycol groups to prevent nonspecific interactions from interfering molecules. Because of their colloidal behavior, the MCSNPs remain in suspension for months without sedimenting. However, because of their low relative magnetic weight (9.5%) and their low volume, the magnetic gradient generated by a single magnet is not sufficient to trap these MCSNPs. To handle such MCSNPs in microdevice, we have recently developed an original design integrating a high magnetic field gradient chamber consisting of ferromagnetic iron beads packed with a physical restriction.[50] When an external permanent magnet is placed on the top of the microdevice, the magnetic field lines are concentrated through the iron beads, thus locally increasing the magnetic force and allowing simple and efficient MCSNPs trapping into the magnetic chamber.

In this work, we combined the benefit of such magnetic trapping with the colloidal behavior of functionalized MCSNPs to perform an original on-chip immunoassay. The microchip potential was first demonstrated with α-lactalbumin (α-lac) as the model antigen (Ag) and anti-α-lac IgG as the model target antibody (AbI). The Ag was grafted on the surface of the MCSNPs (18 Ag/MCSNP) to be used as the capture immunosupport.[45] The immunoassay we developed consists first in the capture of AbI on the nanosupport to form MCSNP–Ag–AbI, this first interaction takes place in the colloidal suspension within the microchip. The MCSNPs are then trapped and preconcentrated into the magnetic chamber. The detection of AbI is then performed in the heterogeneous MCSNPs packed assembly confined in the magnetic chamber, from a second interaction between AbI and a fluorescent-labeled antibody (AbII*). To achieve a high sensitivity, we first evaluated the preconcentration capacity of the magnetic chamber. Using such a magnetic trap,

the amount of confined MCSNPs reached a maximum because of the magnetic chamber saturation, which has been termed the capture capacity (2.2×10^{16} MCSNPs cm^{-3}).[50] It has been demonstrated that MCSNPs concentration (from 6.6×10^{11} to 1×10^{14} MCSNPs mL^{-1}) has an influence on the MCSNPs confinement speed into the magnetic chamber. As expected the higher the MCSNPs concentration, the faster the magnetic chamber saturation was reached. However, even at the lowest MCSNPs concentration, the time required to reach the capture capacity was inferior to 8 min (Fig. 3) while a preconcentration factor of 35 000 is reached.

When developing such an immunoassay, the AbI quantitation relies mainly on the optimization of the AbI capture by the colloidal MCSNPs-Ag suspension during the incubation step because only a fraction (from 0.05 to 7.5% according to MCSNPs concentration) of the total amount of MCSNPs was finally trapped in the magnetic chamber. The MCSNP–Ag/AbI interaction kinetics in the colloidal phase has been studied.[51] We have demonstrated the advantage of using nanosupports compared with micro- and millimetric supports in batch experiments as the decrease in the immunosupport dimension quickens the AbI capture kinetics. This is due to the much higher surface to volume ratio offered by MCSNPs as well as the short interparticular distance that reduces diffusion distances. The capture of AbI by the colloidal suspension of MCSNPs-Ag was described by an adsorption-like kinetic process with an apparent first-order rate constant $k_{app} \approx 10^{-3}$ s^{-1}, which is 10 and 1000 times improved compared to microbeads and microtiter plate support respectively. It was then expected that within 10 min of incubation, the equilibrium capture would be reached and the amount of AbI bound to MCSNPs-Ag was only fixed by the ratio of each candidate. Thus, for a given AbI concentration, the lower the MCSNP–Ag concentration, the higher the proportion of MCSNP–Ag bound to AbI at the end of the incubation step and therefore the higher the amount of AbI trapped in the chamber during the preconcentration step. The effect of the MCSNPs concentration on the fluorescent signal is shown in Fig. 4; the highest fluorescent signals were obtained for the lowest MCSNP concentrations, whereas using the highest MCSNPs concentration resulted in a signal that was not detectable. The immunoassay sensitivity was thus inversely proportional to the MCSNPs-Ag concentration during the MCSNPs-Ag/AbI incubation. It has to be mentioned that AbI capture kinetics were not dependent on MCSNPs concentration (in the range from 10^{11} to 10^{14} MCSNPs mL^{-1}).[51] One can expect that low MCSNPs concentration coupled with high preconcentration would lead to high sensitivity.

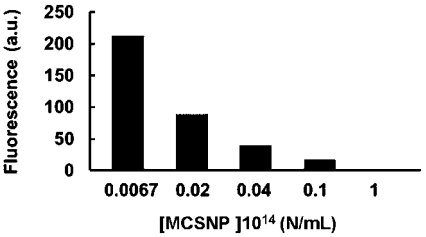

Fig. 4 Influence of the initial MCSNPs concentration on assay sensitivity. Target AbI and AbII* were set at 30 ng mL^{-1} and 100 μg mL^{-1}, respectively. Both AbI and AbII* were incubated at the same time for 2 h in the colloidal phase.

We then evaluated more specifically the advantages of the dedicated microchip for AbI target quantitation in terms of kinetic performances and sensitivity. First, we evaluated the potentiality of the developed microchip for the determination of immunocapture reaction kinetics and wished to compare its kinetic performances to a gold standard, *i.e.*, an immunoassay performed with microtiter plate. Here, the time course of the AbI/AbII* interaction has been investigated using the fluorescent signal from AbII*. As shown in Fig. 2, the MCSNPs-Ag–AbI complex was confined within the magnetic chamber and AbII* was flowed through it, because rinsing and preconcentration steps are required after the AbI capture, particularly when it is present at low concentration in a complex matrix such as serum. As shown in Fig. 5, using the trapped MCSNPs within the magnetic plug, a plateau was reached after only 5 min of incubation, reducing drastically the incubation time compared to the microtiter plate. The AbII* capture in the heterogeneous phase was described by a standard Langmuir-type adsorption process; the apparent first-order kinetic rate constant of the AbI/AbII* interaction was 1000-fold enhanced using the microchip ($k_{app} = 3.5 \times 10^{-2}$ s^{-1}) compared to similar experiments performed with microtiter plate ($k_{app} = 5 \times 10^{-5}$ s^{-1}). These results were related to the increase in the confined AbI concentration because of the magnetic trapping of MCSNP-Ag–AbI. The kinetic improvement of each incubation step allows the entire assay to be performed within 20 min in the microchip, whereas 6 h is required using the microtiter plate.

We next evaluated the sensitivity from the microchip immunoassay devoted to AbI quantitation. In order to compare the

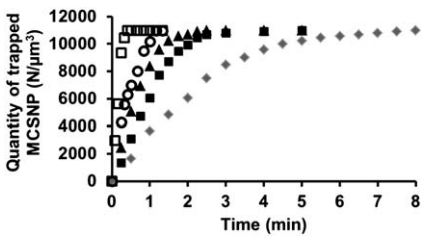

Fig. 3 Influence of the initial MCSNPs concentration on the MCSNPs capture kinetics in the magnetic chamber for five different concentrations: 6.7×10^{11} (◆), 2×10^{12} (■), 4×10^{12} (▲), 1×10^{13} (○) and 1×10^{14} MCSNP mL^{-1} (□).

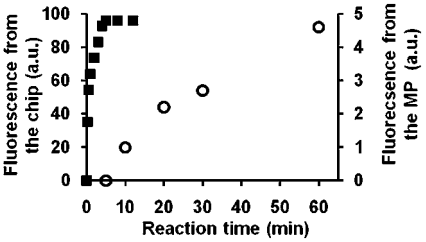

Fig. 5 Interaction kinetics between target AbI and AbII* using the chip (■) or the microtiter plate (○). Target AbI (10 min in the chip and 2 h incubation in the microtiter plate) and AbII* were set at 30 ng mL^{-1} and 100 μg mL^{-1}, respectively. MP: microtiter plate.

limit of detection (LOD) achieved using a microchip and microtiter plate, the same immunological partners were used. On the basis that a significant signal is three standard deviations above the control, the limit of detection was about 1 ng mL^{-1} using the chip and 30 ng mL^{-1} with the conventional microtiter plate, thus highlighting the sensitivity gain achieved using the microchip (Fig. 6). These results also underlined that using the conventional microtiter plate, a catalytic amplification (ELISA) using phosphatase alkaline labeled antibody was necessary (Fig. S1 in the ESI†) to meet the sensitivity required for allergy diagnosis (ranging from 1 ng mL^{-1} to 200 ng mL^{-1}), whereas signal amplification can be avoided with the microfluidic approach. Moreover, the very low fluorescent signal measured in the absence of AbI underlined the assay specificity. The assay specificity was optimized using a buffer of high ionic strength (150 mM) and PEG group density at the nanoparticles surface. These conditions have been previously discussed.[50]

To further investigate the advantage of using a colloidal suspension as immunosupport for the AbI capture, a second approach has been carried out in which MCSNPs-Ag were initially confined in the magnetic chamber before the immunological reaction. We then performed both the Ag/AbI and AbI/AbII* interactions successively within the packed bed of MCSNPs-Ag. In this case, the LOD achieved was of the same order of magnitude as the value obtained using the conventional microtiter plate (Fig. 5). These results demonstrated that colloidal suspension may favor diffusion of the immunological partners as well as Ag accessibility, thus improving AbI capture during the first incubation. Indeed previous numerical simulations have shown that MCSNPs-Ag were concentrated and localized at iron beads pole in the magnetic chamber.[50] In that way a part of the Ag was not accessible thus reducing the quantity of the captured AbI. The combination of MCSNPs and the microdevice presents three major advantages over the conventional microtiter plate: the LOD was 30-fold improved with a 20-fold time saving and the reagent consumption was about 5 μL compared with the 200 μL required for each microtiter plate well. The low volume of serum required is a particular key issue when dealing with milk allergy, because it mainly concerns infants and young children whose sera are extremely precious.

We finally applied the chip to milk allergy diagnosis in real sera samples (Fig. 7). The diagnosis was based on the determination of specific IgE directed against one milk allergen (α-lac). The determination of anti-α-lac IgE from three different sera was first evaluated by ELISA in microtiter plates using phosphatase alkaline labeled anti-IgE as the detecting antibody since enzymatic amplification is required to reach the sensitivity as mentioned previously. The anti-α-lac IgE concentration was estimated to be 4.5 and 24 ng mL^{-1} for fivefold diluted sera 1 and 2, respectively. Similar experiments were performed using the chip following the protocol depicted in Fig. 2 and described in the Materials and methods section. With this format, the detection was based on fluorescence measurement using FITC labeled anti-IgE. A healthy patient serum was used as the negative control (without anti-α-lac IgE); as expected, it produces a lower signal than the sera of the two allergic patients. Moreover, IgE concentrations from sera 1 and 2 were distinguished and

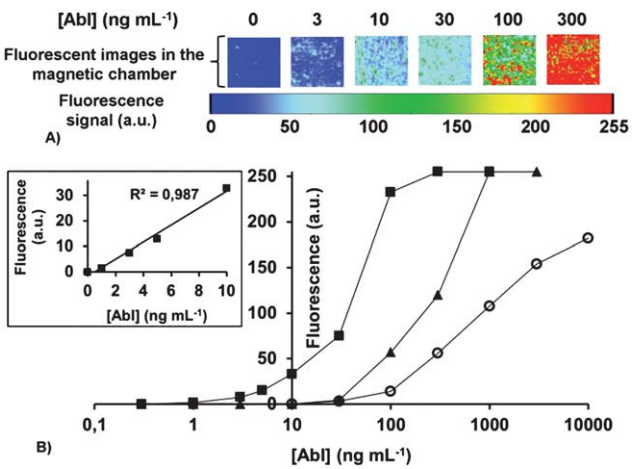

Fig. 6 (A) An example of the AbI concentration influence on the fluorescence signal in the magnetic chamber. (B) Calibration curve of AbI using the microtiter plate (○) or the chip in two different approaches: AbI and AbII* capture occurred successively in the heterogeneous phase (▲) or AbI capture occurred in the colloidal phase and AbII* capture occurred in the heterogeneous phase (■). AbI was incubated for 5 min in the chip and for 2 h in the microtiter plate. AbII* was set at 100 μg mL^{-1} for 5 and 60 min incubation in the chip and the microtiter plate, respectively, see details in the ESI†. The inset is a focus on 0–10 ng mL^{-1} AbI concentration when the AbI capture occurred in the colloidal phase; the plots revealed a good linearity. The response was linear on 1–30 ng mL^{-1} for ■, 30–300 ng mL^{-1} for ▲ and 30–1000 ng mL^{-1} for ○.

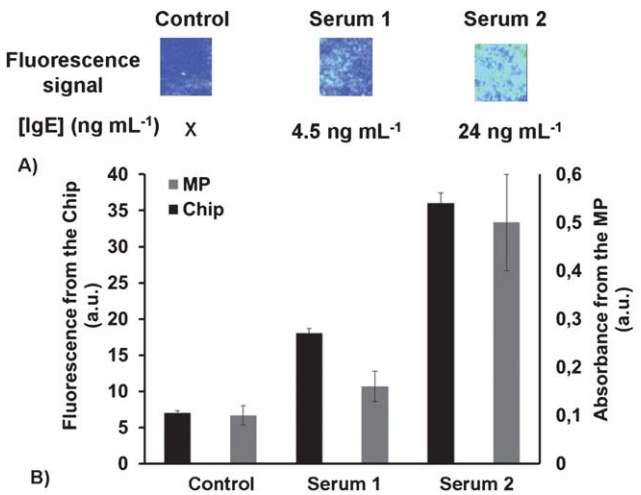

Fig. 7 (A) Fluorescent images observed in the chip for three different sera. (B) Fluorescence and absorbance intensity measured from the chip and the microtiter plate, respectively, for the three tested sera. The diagnosis in the chip was performed as depicted in Fig. 2. The sera were incubated for 5 min in the chip and 3 h in the microtiter plate. Then, after the washing step, the detecting Ab (labeled with FITC or enzyme for the chip and microtiter plate, respectively) was incubated for 5 min in the chip and 2 h in the microtiter plate. The detection in the microtiter plate was performed by adding an enzyme substrate for 30 min and the intensity was read at 405 nm. The relative standard deviation (three repetitions) was 2.7% with the chip and 12% with the microtiter plate, see details in the ESI†. MP: microtiter plate.

exhibited the same tendency as those obtained with ELISA in a microtiter plate. These results underline the clinical applicability of this nanoparticle-based chip for allergy diagnosis, as well as its compatibility with complex biological samples.

Conclusion

In this work we have demonstrated a new microchip approach integrating MCSNPs to perform fast and sensitive immunoassay. This chip takes advantage of diffusing MCSNPs used as immunosupport to improve the target analyte capture kinetics as well as a magnetic chamber that allows target preconcentration to achieve a higher sensitivity than that observed in a standard microtiter plate. The integrated steps of target capture, preconcentration and detection were completed in a shortened analysis time with a reduced sample consumption compared to the immunoassay performed in the microtiter plate. We then demonstrated that the developed chip could be successfully applied to an easy and rapid allergy diagnosis by quantifying specific IgE from patient sera. It is envisioned that this system could integrate multiplexing using different functionalized NPs as well as automation.

Acknowledgements

This work was supported by the French research agency ANR SOLUDIAG ANR-07-BLAN-02660. The authors thank Pascal Poncet and Hélène Sénéchal for helpful discussion.

References

1 J. Paupe, E. Paty, J. de Blic and P. Scheinmann, *Rev. Fr. Allergol. Immunol. Clin.*, 2001, **41**, 424–436.
2 *Middleton's Allergy Principles and Practice*, ed. N. Franklin Adkinson, *et al.*, Elsevier, 7 edn, 2008.
3 M. Cretich, G. Di Carlo, C. Giudici, S. Pokoj, I. Lauer, S. Scheurer and M. Chiari, *Proteomics*, 2009, **9**, 2098–2107.
4 H. Y. Li, V. Dauriac, V. Thibert, H. Senechal, G. Peltre, X. X. Zhang and S. Descroix, *Lab Chip*, 2010, **10**, 2597–2604.
5 S. Cesaro-Tadic, G. Dernick, D. Juncker, G. Buurman, H. Kropshofer, B. Michel, C. Fattinger and E. Delamarche, *Lab Chip*, 2004, **4**, 563–569.
6 T. G. Henares, F. Mizutani and H. Hisamoto, *Anal. Chim. Acta*, 2008, **611**, 17–30.
7 A. T. Pereira, P. Novo, D. M. F. Prazeres, V. Chu and J. P. Conde, *Biomicrofluidics*, 2011, **5**, 014102.
8 O. Hofmann, G. Voirin, P. Niedermann and A. Manz, *Anal. Chem.*, 2002, **74**, 5243–5250.
9 J. P. Golden, T. M. Floyd-Smith, D. R. Mott and F. S. Ligler, *Biosens. Bioelectron.*, 2007, **22**, 2763–2767.
10 V. N. Morozov, S. Groves, M. J. Turell and C. Bailey, *J. Am. Chem. Soc.*, 2007, **129**, 12628–12629.
11 D. Holmes, J. K. She, P. L. Roach and H. Morgan, *Lab Chip*, 2007, **7**, 1048–1056.
12 M. Herrmann, T. Veres and M. Tabrizian, *Lab Chip*, 2006, **6**, 555–560.
13 E. Verpoorte, *Lab Chip*, 2003, **3**, 60N.
14 M. Ikami, A. Kawakami, M. Kakuta, Y. Okamoto, N. Kaji, M. Tokeshi and Y. Baba, *Lab Chip*, 2010, **10**, 3335–3340.
15 K. Sato, M. Yamanaka, T. Hagino, M. Tokeshi, H. Kimura and T. Kitamori, *Lab Chip*, 2004, **4**, 570–575.
16 C. A. Marquette and L. J. Blum, *Anal. Bioanal. Chem.*, 2008, **390**, 155–168.
17 J. Do and C. H. Ahn, *Lab Chip*, 2008, **8**, 542–549.
18 K. S. Kim and J.-K. Park, *Lab Chip*, 2005, **5**, 657–664.
19 F. Lacharme, C. Vandevyver and M. A. M. Gijs, *Microfluid. Nanofluid.*, 2009, **7**, 479–487.
20 S. A. Peyman, A. Iles and N. Pamme, *Lab Chip*, 2009, **9**, 3110–3117.
21 R. S. Sista, A. E. Eckhardt, V. Srinivasan, M. G. Pollack, S. Palanki and V. K. Pamula, *Lab Chip*, 2008, **8**, 2188–2196.
22 Y.-F. Lee, K.-Y. Lien, H.-Y. Lei and G.-B. Lee, *Biosens. Bioelectron.*, 2009, **24**, 745–752.
23 S. Pal and E. C. Alocilja, *Biosens. Bioelectron.*, 2009, **24**, 1437–1444.
24 X. Cao, Y. Ye and S. Liu, *Anal. Biochem.*, 2011, **417**, 1–16.
25 Y.-J. Liu, D.-J. Yao, H.-Y. Chang, C.-M. Liu and C. Chen, *Biosens. Bioelectron.*, 2008, **24**, 558–565.
26 B.-H. Liu, Z.-J. Tsao, J.-J. Wang and F.-Y. Yu, *Anal. Chem.*, 2008, **80**, 7029–7035.
27 L. Potůčková, F. Franko, M. Bambousková and P. Dráber, *J. Immunol. Methods*, 2011, **371**, 38–47.
28 J. B.-H. Tok, F. Y. S. Chuang, M. l. C. Kao, K. A. Rose, S. S. Pannu, M. Y. Sha, G. Chakarova, S. G. Penn and G. M. Dougherty, *Angew. Chem., Int. Ed.*, 2006, **45**, 6900–6904.
29 S. R. Nicewarner-Peña, A. J. Carado, K. E. Shale and C. D. Keating, *J. Phys. Chem. B*, 2003, **107**, 7360–7367.
30 S. R. Nicewarner-Peña, R. G. Freeman, B. D. Reiss, L. He, D. J. Pena, I. D. Walton, R. Cromer, C. D. Keating and M. J. Natan, *Science*, 2001, **294**, 137–141.
31 Y. Cui, Q. Wei, H. Park and C. M. Lieber, *Science*, 2001, **293**, 1289–1292.
32 C. R. Martin, *Science*, 1994, **266**, 1961–1966.
33 D. Tang, Y. Yu, R. Niessner, M. Miró and D. Knopp, *Analyst*, 2010, **135**, 2661–2667.
34 Y. Weizmann, F. Patolsky, E. Katz and I. Willner, *J. Am. Chem. Soc.*, 2003, **125**, 3452–3454.
35 S. Mayilo, M. A. Kloster, M. Wunderlich, A. Lutich, T. A. Klar, A. Nichtl, K. Krzinger, F. D. Stefani and J. Feldmann, *Nano Lett.*, 2009, **9**, 4558–4563.
36 X. Liu, Q. Dai, L. Austin, J. Coutts, G. Knowles, J. Zou, H. Chen and Q. Huo, *J. Am. Chem. Soc.*, 2008, **130**, 2780–2782.
37 F. Destremaut, J.-B. Salmon, L. Qi and J.-P. Chape, *Lab Chip*, 2008, **8**, 950–957.
38 K. F. Lei and Y. K. C. Butt, *Microfluid. Nanofluid.*, 2010, **8**, 131–137.
39 Y. Lu, W. Shi, J. Qin and B. Lin, *Electrophoresis*, 2009, **30**, 579–582.
40 M.-I. Mohammed and M. P. Y. Desmulliez, *Lab Chip*, 2011, **11**, 569–595.
41 W. Chen, C. Peng, Z. Jin, R. Qiao, W. Wang, S. Zhu, L. Wang, Q. Jin and C. Xu, *Biosens. Bioelectron.*, 2009, **24**, 2051–2056.
42 J. C. McDonald and G. M. Whitesides, *Acc. Chem. Res.*, 2002, **35**, 491–499.
43 J. C. McDonald, D. C. Duffy, J. R. Anderson, D. T. Chiu, H. K. Wu, O. J. A. Schueller and G. M. Whitesides, *Electrophoresis*, 2000, **21**, 27–40.
44 V. Maurice, T. Georgelin, J.-M. Siaugue and V. Cabuil, *J. Magn. Magn. Mater.*, 2009, **321**, 1408–1413.
45 B. Teste, J. Vial, S. Descroix, T. Georgelin, J.-M. Siaugue, J. Petr, A. Varenne and M.-C. Hennion, *Talanta*, 2010, **81**, 1703–1710.
46 F. d'Orlyé, A. Varenne, T. Georgelin, J.-M. Siaugue, B. Teste, S. Descroix and P. Gareil, *Electrophoresis*, 2009, **30**, 2572–2582.
47 J. Petr, B. Teste, S. Descroix, J.-M. Siaugue, P. Gareil and A. Varenne, *Electrophoresis*, 2010, **31**, 2754–2761.
48 S. Krishnamurthy, P. Bhattacharya and P. E. Phelan, *Nano Lett.*, 2006, **6**, 419–423.
49 T. Georgelin, S. Bombard, J.-M. Siaugue and V. Cabuil, *Angew. Chem., Int. Ed.*, 2010, **49**, 8897–8901.
50 B. Teste, F. Malloggi, A.-L. Gassner, T. Georgelin, J.-M. Siaugue, A. Varenne, H. Girault and S. Descroix, *Lab Chip*, 2011, **11**, 833–840.
51 B. Teste, F. Kanoufi, S. Descroix, P. Poncet, T. Georgelin, J.-M. Siaugue, J. Petr, A. Varenne and M.-C. Hennion, *Anal. Bioanal. Chem.*, 2011, **400**, 3395–3497.